www.nature.com/cdd

CDDpress

ARTICLE

Check for updates

Transglutaminase 2 crosslinks zona pellucida glycoprotein 3 to prevent polyspermy

Zhaokang Cui[1,3], Yajuan Lu[1,2,3], Yilong Miao[1,3], Xiaoxin Dai[1], Yu Zhang[1] and Bo Xiong[1]✉

Soon after fertilization, the block mechanisms are developed in the zona pellucida (ZP) and plasma membrane of the egg to prevent any additional sperm from binding, penetration, and fusion. However, the molecular basis and underlying mechanism for the post-fertilization block to sperm penetration through ZP has not yet been determined. Here, we find that transglutaminase 2 (Tgm2), an enzyme that catalyzes proteins by the formation of an isopeptide bond within or between polypeptide chains, crosslinks zona pellucida glycoprotein 3 (ZP3) to result in the ZP hardening after fertilization and thus prevents polyspermy. Tgm2 abundantly accumulates in the subcortical region of the oocytes and vanishes upon fertilization. Both inhibition of Tgm2 activity in oocytes by the specific inhibitor in vitro and genetic ablation of Tgm2 in vivo cause the presence of additional sperm in the perivitelline space of fertilized eggs, consequently leading to the polyploid embryos. Biochemically, recombinant Tgm2 binds to and crosslinks ZP3 proteins in vitro, and incubation of oocytes with recombinant Tgm2 protein inhibits the polyspermy. Altogether, our data identify Tgm2 as a participant of zona block to the post-fertilization sperm penetration *via* hardening ZP surrounding fertilized eggs, extending our current understanding about the molecular basis of block to polyspermy.

Cell Death & Differentiation (2022) 29:1466–1473; https://doi.org/10.1038/s41418-022-00933-0

INTRODUCTION

Monospermic fertilization in mammals is a complicated event in sexual reproduction that requires the orderly interaction between haploid sperm and egg to create a new, genetically distinct, diploid organism [1, 2]. Sperm, capacitated by passage through the female reproductive tract, encounter ovulated eggs in the ampulla of the oviduct. After penetration through the cumulus mass, sperm bind the extracellular zona pellucida (ZP) that surrounds ovulated eggs. The ZP of humans is composed of four (ZP1-4) and that of mouse three (ZP1-3) glycoproteins. Subsequent sperm penetration through the zona matrix and gamete fusion results in fertilization [3–6]. Once fertilized, both plasma membrane and ZP are biochemically altered, rendering the egg unreceptive to additional sperm and thereby reducing the chances of creating nonviable polyploid embryos [7]. To prevent polyspermy, three post-fertilization block mechanisms are developed in mammalian oocytes [8]. The first two occur immediately after fertilization and prevent additional sperm from fusing with the fertilized egg's plasma membrane as well as penetrating the extracellular ZP [9]. The third and definitive block occurs over several hours and ensures that sperm do not bind to the surface of the ZP [10]. The rapid post-fertilization shedding of Juno (Folr4, folate receptor 4), a receptor for the sperm fusion protein Izumo1 on the egg, from the plasma membrane is responsible for the membrane block to polyspermy [11]. The exocytosis of a zinc metalloprotease ovastacin from cortical granules following fertilization to cleave ZP2 prevents the additional sperm binding to the surface of the ZP surrounding fertilized eggs [12–14]. However, the molecular basis of the ZP block to sperm penetration remains elusive.

MATERIALS AND METHODS

Mouse oocyte and embryo collection and culture

Animal experimental procedures in our study were approved by the Animal Ethics Committee of Nanjing Agricultural University, China, and all mice were housed under the standard specific pathogen-free (SPF) conditions of Animal Core Facility. Briefly, mice were maintained at the controlled condition of temperature (20–23 °C) and illumination (12 h light-dark cycle), and had free access to food and water throughout the period of the study. Fully-grown GV (germinal vesicle) oocytes arrested at prophase of meiosis I from 6–8-week-old C57BL/6 female mice were collected from ovaries in M2 medium (Sigma-Aldrich, St. Louis, MO, USA) at 48 h post-injection of 5 IU pregnant mare serum gonadotropin (PMSG), and cultured further in M16 medium (Sigma-Aldrich) under liquid paraffin oil at 37 °C in an atmosphere of 5% CO_2 incubator to different developmental stages. Ovulated oocytes and embryos from 6~8-week-old female mice were collected before and after mating, respectively, in M2 medium after injection of 5 IU of PMSG followed by 5 IU of human chorionic gonadotropin (hCG) 46–48 h later. Embryos were subsequently cultured in KSOM at 37 °C in 5% CO_2 to obtain 1-cell and 2-cell embryos.

Antibodies

Rabbit polyclonal anti-Tgm2 antibody was made by Zoonbio Biotech (Nanjing, China); rabbit polyclonal anti-ZP3, anti-NSF, and anti-Snap23 antibodies were purchased from Proteintech (Rosemont, IL, USA; 21279-1-AP, 21172-1-AP,

[1]College of Animal Science and Technology, Nanjing Agricultural University, Nanjing 210095, China. [2]Institute of Reproductive Medicine, School of Medicine, Nantong University, Nantong 226019, China. [3]These authors contributed equally: Zhaokang Cui, Yajuan Lu, Yilong Miao. ✉email: xiongbo@njau.edu.cn

Edited by M Piacentini

Received: 17 September 2021 Revised: 17 December 2021 Accepted: 28 December 2021
Published online: 11 January 2022

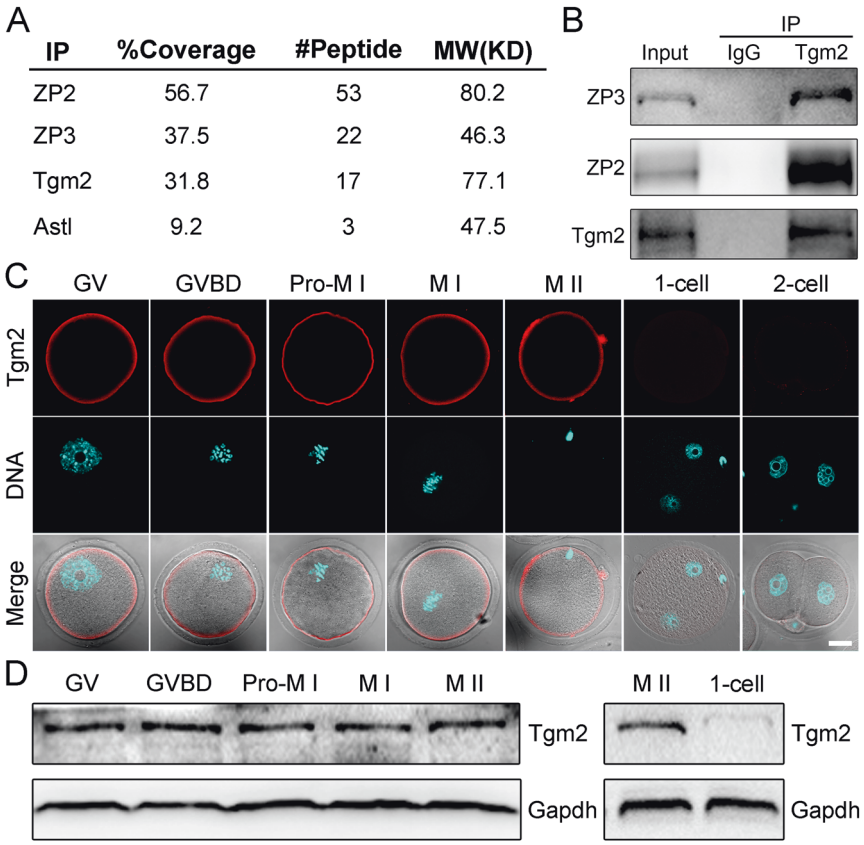

Fig. 1 Tgm2 is a ZP binding protein. A Identification of binding partners of ZP2 by IP and MS analysis. The protein coverage, the number of peptides, and the relative molecular mass were shown for each protein. Astl, astacin like metalloendopeptidase, encoding ovastacin. **B** Co-IP was performed with Tgm2 antibody to validate the interaction between Tgm2 and ZP2/ZP3 in oocytes. The blots of IP eluates were immunoblotted for Tgm2, ZP2, and ZP3, respectively. **C** Localization of Tgm2 in oocytes and embryos. Mouse oocytes and embryos at different developmental stages were immunostained with Tgm2 antibody and counterstained with Hoechst. Scale bar, 20 μm. **D** Protein levels of Tgm2 in oocytes and embryos at different developmental stages. The blots were immunoblotted for Tgm2 and Gapdh, respectively.

10825-1-AP); rat monoclonal anti-ZP2 antibody and rabbit polyclonal anti-ovastacin antibody were obtained from Dr. Jurrien Dean's lab; rabbit monoclonal anti-Gapdh, anti-HA and anti-His antibodies were purchased from Cell Signaling Technology (Danvers, MA, USA; 5174S, 3724S, 12698).

Immunofluorescence and confocal microscopy

Oocytes were fixed in 4% paraformaldehyde/PBS (pH 7.4) for 30 min and permeabilized in 0.5% Triton X-100/PBS for 20 min at room temperature. Then, oocytes were blocked with 1% BSA/PBS for 1 h and incubated with anti-Tgm2 (1:100), or anti-HA (1:100) antibodies at 4 °C overnight. After washing four times (5 min each) in PBS containing 1% Tween 20 and 0.01% Triton X-100, oocytes were incubated with the corresponding secondary antibodies for 1 h and counterstained with Hoechst 33342 (10 μg/ml) for 10 min at room temperature. Finally, oocytes were mounted on glass slides and imaged under a confocal laser scanning microscope (LSM 900 META, Zeiss).

Immunoprecipitation and immunoblotting analysis

Immunoprecipitation was carried out using 800 mouse M II oocytes or 2 μg recombinant proteins according to the manufacturer's instruction for ProFound Mammalian Co-Immunoprecipitation kit (ThermoFisher Scientific).

For immunoblotting, a pool of 200 oocytes or embryos was lysed in 4 × LDS sample buffer (ThermoFisher Scientific) containing the protease inhibitor, separated on 10% Bis-Tris precast gels, and transferred onto PVDF membranes. The blots were blocked in TBST containing 5% low fat dry milk for 1 h at room temperature and then incubated with anti-Tgm2 antibody (1:1000), anti-ZP2 antibody (1:1000), anti-ZP3 antibody (1:1000), anti-ovastacin antibody (1:1000) or anti-Gapdh antibody (1:5000) at 4 °C overnight. After three times of washes in TBST, the blots were incubated with 1:10,000 dilution of HRP (horse radish peroxidase) conjugated secondary antibodies for 1 h at room temperature. Chemiluminescence signals were detected with ECL Plus Western Blotting Substrate (ThermoFisher) and protein bands were acquired by Tanon-3900 Imaging System.

LC-MS/MS and data analysis

The peptide samples were dissolved in 2% acetonitrile/0.1% formic acid and analyzed using TripleTOF 5600 plus mass spectrometer coupled with the Eksigent nanoLC System (SCIEX, USA). The peptide was loaded onto a C18 trap column (5 μm, 100 μm × 20 mm), and eluted at 300 nL/min onto a C18 analytical column (3 μm, 75 μm × 150 mm) over a 60 min gradient. The two mobile phases were buffered A (2% acetonitrile/0.1% formic acid/98% H_2O) and buffer B (98% acetonitrile/0.1% formic acid/2% H_2O). For IDA (information-dependent acquisition), survey scans were acquired in 250 ms and 40 product ion scans were collected in 50 ms/per scan. MS1 spectra were collected in the range 350–1500 m/z, and MS2 spectra were collected in the range of 100–1500 m/z. Precursor ions were excluded from reselection for 15 s.

Protein identification was achieved by searching the obtained MS spectra files using software ProteinPilot 4.5 Software (July 2012; AB SCIEX) against a database from uniprot mouse protein sequencing data. All identified proteins had an Unused Protscore of >1.3 (which corresponds to proteins identified with >95% confidence), and proteins with 1 unique peptides were considered confidently identified.

Establishment of *Tgm2*$^{-/-}$ mice by CRISPR/Cas9

pMLM3613 (Addgene, Cambridge, MA) expressing Cas9 was linearized by PmeI (New England Biolabs, Ipswich, MA, USA), purified with a PCR clean-up kit (Macherey-Nagel, Duren, Germany), and in vitro transcribed with mMESSAGE mMACHINE T7 ULTRA Transcription kit (ThermoFisher Scientific, Waltham, MA, USA). Double-stranded synthetic DNA oligo targeting exon 2 of *Tgm2* (5′-TAGGCGTCGTGGTCAGCGCTTC-3′) was cloned into the pair of BsaI sites of pDR274 (Addgene) expressing sgRNA. After linearization by

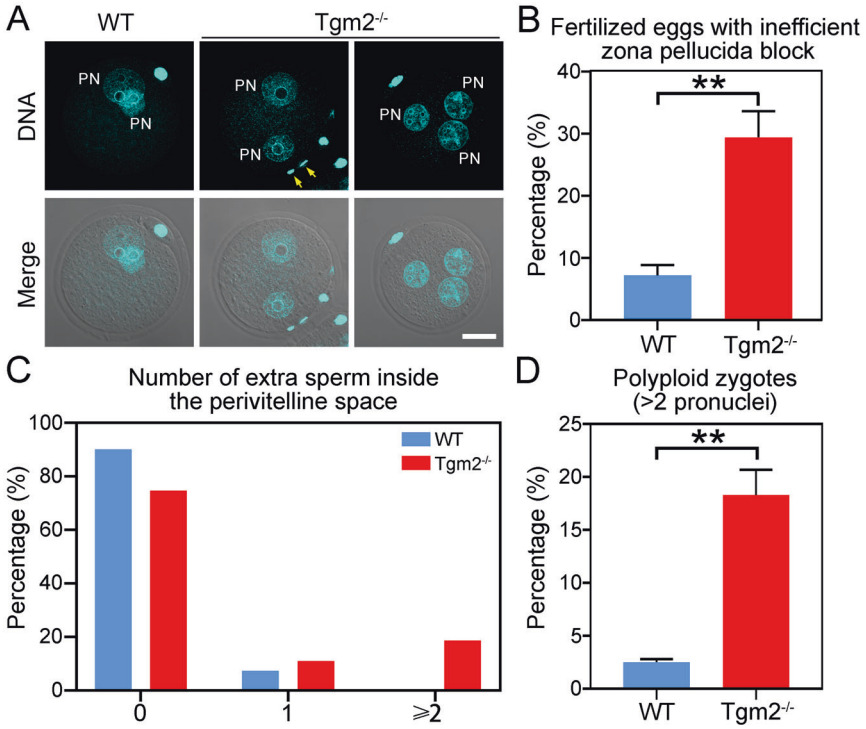

Fig. 2 Genetic ablation of Tgm2 impairs the ZP block to polyspermy in vivo. A Representative images of in vivo fertilized oocytes in WT and *Tgm2*-null groups. Fertilized oocytes were stained with Hoechst to display the pronuclei and extra sperm (arrows) in the perivitelline space. Scale bar, 20 μm. **B** The rate of fertilized oocytes with extra sperm in the perivitelline space was quantified in WT ($n = 300$) and *Tgm2*-null ($n = 328$) groups. **C** The number of extra sperm in the perivitelline space of fertilized oocytes was counted in WT ($n = 300$) and *Tgm2*-null ($n = 328$) groups. **D** The rate of polyploid zygotes was quantified in WT ($n = 300$) and *Tgm2*-null ($n = 328$) groups. Data of (B) and (D) were presented as mean percentage (mean ± SEM) of at least three independent experiments. $^{**}P < 0.01$.

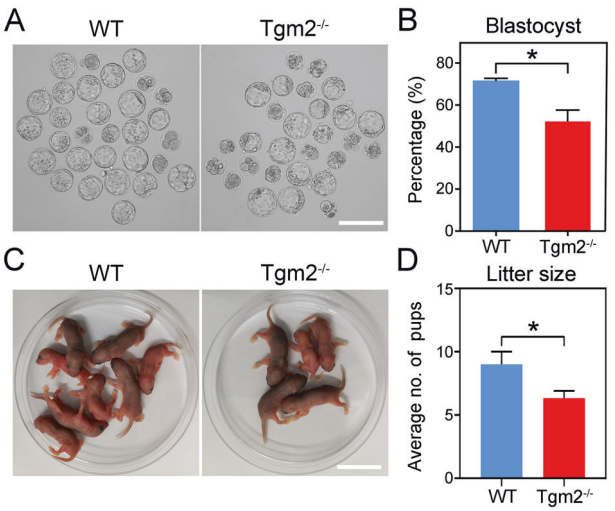

Fig. 3 Genetic ablation of Tgm2 weakens the female fertility. A Representative images of blastocysts developed in vitro from zygotes in WT and *Tgm2*-null groups. WT or *Tgm2*-null female mice were mated with WT male mice to obtain zygotes which were then cultured to blastocysts in vitro. Scale bar, 200 μm. **B** The rate of blastocyst formation was quantified in WT ($n = 218$) and *Tgm2*-null ($n = 186$) groups. **C** Representative images of pups delivered by WT and *Tgm2*-null female mice which were mated with WT male mice. **D** The average number of pups delivered by per female mouse was quantified in WT ($n = 5$) and *Tgm2*-null ($n = 5$) groups. The female mice were co-caged with fertile male mice for at least 6 months. Data of (**B**) and (**D**) were presented as mean percentage of value (mean ± SEM) of at least three independent experiments. $^{*}P < 0.05$.

digestion with DraI, the plasmid was purified with the PCR clean-up kit and in vitro transcribed using MEGAshortscript T7 Transcription kit (ThermoFisher Scientific). After transcription, the Cas9 cRNA and the sgRNA were purified with MEGAclear kit (ThermoFisher Scientific) according to the manufacturer's instruction and eluted in RNase-free water.

For zygote injection, one-cell embryos were collected from B6D2F1 female mice which were mated with B6D2F1 males and injected with the mixture of Cas9 cRNA (50 ng/μl) and sgRNA (20 ng/μl). The injected embryos were cultured in KSOM (EMD Millipore, Billerica, MA, USA) until the blastocyst stage and transferred into pseudopregnant ICR female mice. The genotype of the *Tgm2*-null allele was initially determined by the DNA sequence of tail DNA and subsequently by PCR using an oligonucleotide primer that bridged the deleted sequence.

Sperm binding assay and In vitro fertilization

Sperm was released from the cauda epididymides of male mice (3–6-month-old) with proven fertility in human tubal fluid (HTF) medium and capacitated for 1 h at 37 °C in 5% CO_2. Ovulated oocytes were harvested as described above. For sperm binding assay, 4×10^5/mL capacitated sperm were incubated with ovulated oocytes in 100 μL HTF for 1 h at 37 °C in a humidified atmosphere of 5% CO_2. Sperm binding to ovulated oocytes was observed using capacitated sperm and 2-cell embryos as a negative wash control. Samples were fixed in 4% PFA for 30 min, stained with Hoechst 33342. Bound sperm were quantified from z projections acquired by a confocal microscope. For insemination, 4×10^5/mL capacitated sperm were incubated with ovulated oocytes in 100 μL HTF for 6–8 h at 37 °C in a humidified atmosphere of 5% CO_2. The presence of pronuclei was scored as successful fertilization.

cRNA construct and in vitro transcription

Wild-type Tgm2 cDNA was sub-cloned into pcDNA3.1/6×HA vector. Capped cRNA was synthesized from linearized plasmid using mMESSAGE mMACHINE T7 ULTRA Transcription kit (ThermoFisher Scientific) and purified with MEGAclear kit (ThermoFisher Scientific). GV oocytes were microinjected with 10–12 pl of 1 μg/μl cRNA in M2 medium containing

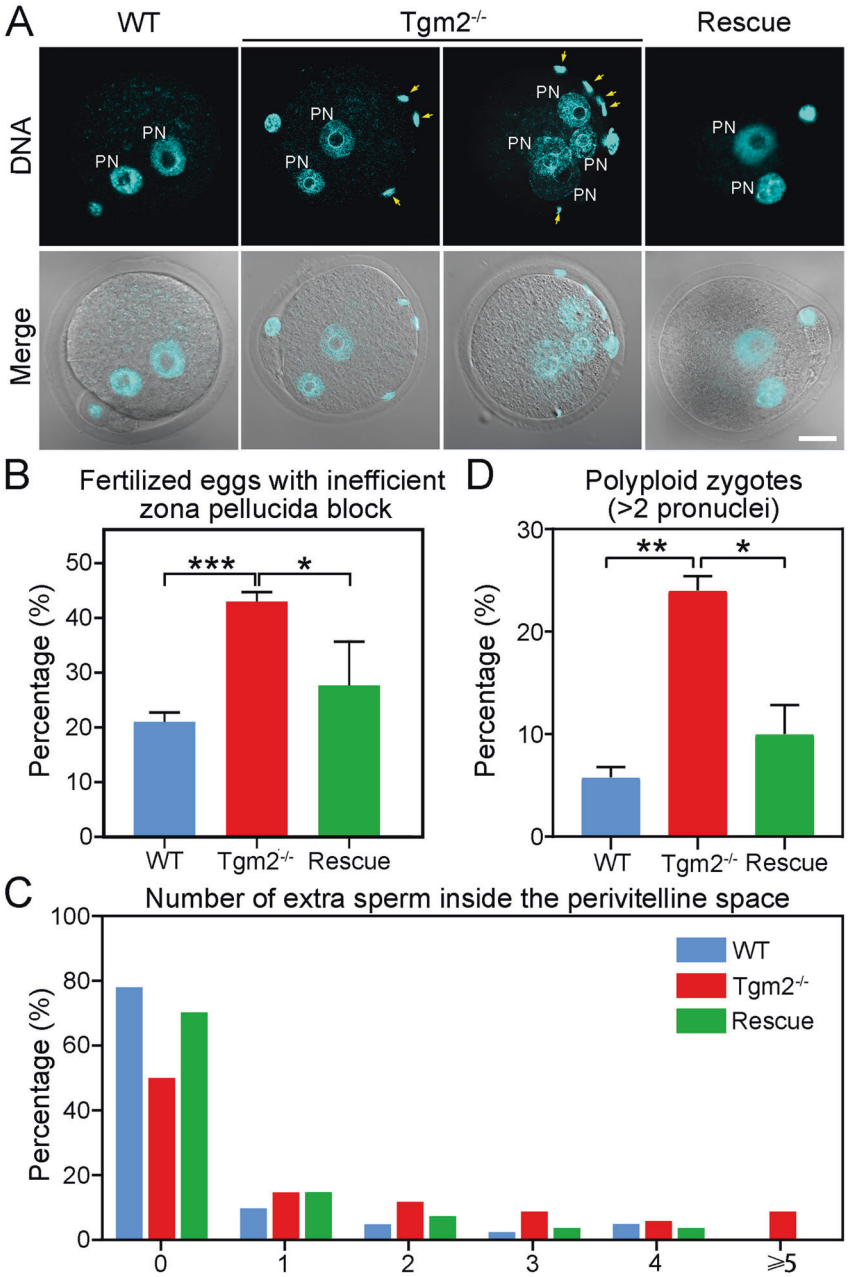

Fig. 4 Genetic ablation of Tgm2 compromises the ZP block to polyspermy in vitro. A Representative images of in vitro fertilized oocytes in WT, *Tgm2*-null, and rescue (*Tgm2*-null + Tgm2-6 × HA cRNA) groups. Fertilized oocytes were stained with Hoechst to display the pronuclei and extra sperm (arrows) in the perivitelline space. Scale bar, 20 μm. **B** The rate of fertilized oocytes with extra sperm in the perivitelline space was quantified in WT ($n = 332$), *Tgm2*-null ($n = 340$) and rescue ($n = 324$) groups. **C** The number of extra sperm in the perivitelline space of fertilized oocytes was counted in WT ($n = 332$), *Tgm2*-null ($n = 340$) and rescue ($n = 324$) groups. **D** The rate of polyploid zygotes was quantified in WT ($n = 332$), *Tgm2*-null ($n = 340$) and rescue ($n = 324$) groups. Data of (**B**) and (**D**) were presented as mean percentage (mean ± SEM) of at least three independent experiments. $^{*}P < 0.05$, $^{**}P < 0.01$, $^{***}P < 0.001$.

2.5 μM milrinone and then incubated for 4 h, allowing enough time for translation, followed by releasing into milrinone-free M16 medium for further culture. Ovulated oocytes were microinjected with cRNA in M2 medium and then incubated in HTF medium for 4 h, followed by IVF.

SiRNA knockdown

Snap23-targeting siRNA oligo (Genepharma, Shanghai, China; antisense sequence: 5′-UUAAAGUCUUCUCUGCCUCTT-3′) or ovastacin-targeting siRNAoligo (Genepharma, antisense sequence: 5′-UAAUGUGACUUCCAGG UGCTT-3′) was diluted with water to give a working concentration of 25 μM, and then approximately 5–10 pl of oligo was microinjected into the cytoplasm of fully grown GV oocytes using a Narishige microinjector (Tokyo, Japan). In order to facilitate the degradation of mRNA by siRNA, oocytes were arrested at GV stage in M16 medium containing 2.5 μM milrinone for 24 h, and then transferred to milrinone-free M16 medium to resume the meiosis for subsequent experiments.

Purification of His-tagged proteins

Target proteins were obtained in the form of intracellular expression through baculovirus-insect cell protein expression system. Briefly, Tgm2, ZP2, and ZP3 cDNA were sub-cloned into pFastBac1 vector, respectively. After transformation, the recombinant bacmids were selected by blue-white screening method. Following PCR identification, Sf9 cells were transfected with bacmids to obtain P1 and P2 generation viruses. 0.5 L Sf9

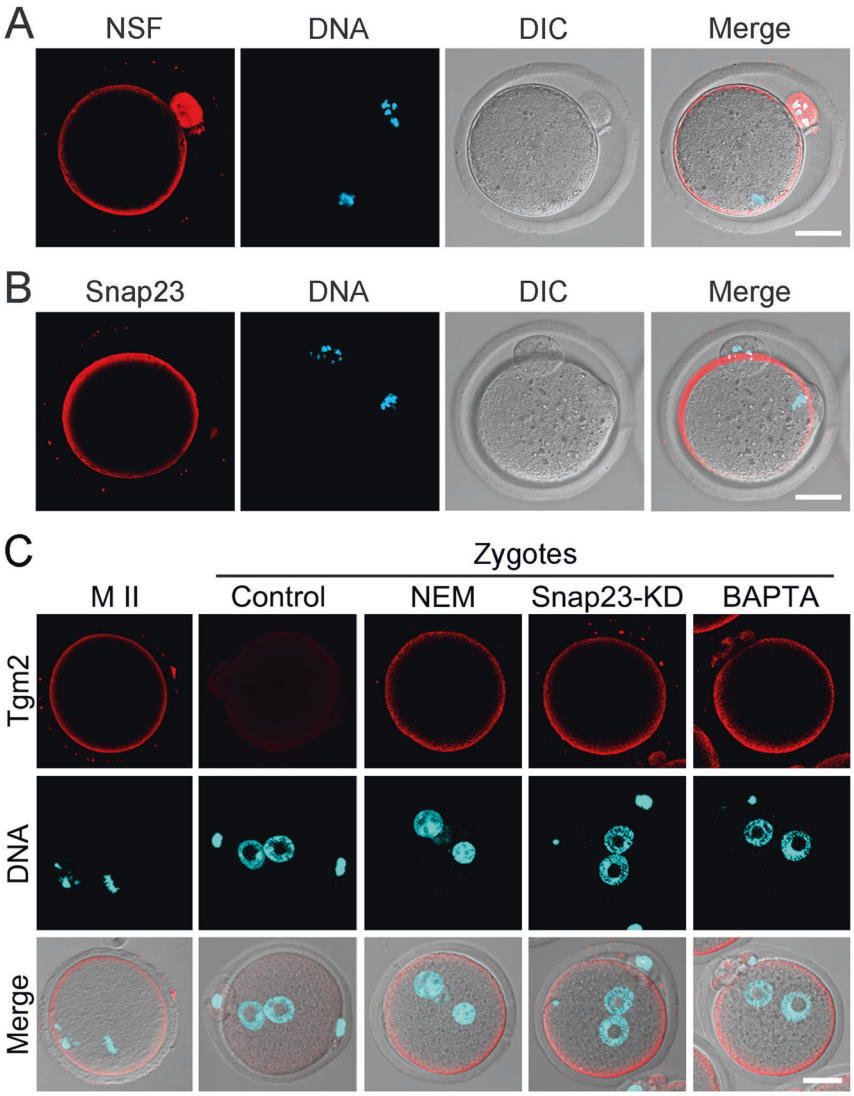

Fig. 5 Exocytosis of Tgm2 triggered by fertilization is mediated by SNARE pathway. A Subcellular localization of NSF in M II oocytes. Oocytes were immunostained with NSF antibody and counterstained with Hoechst. Scale bar, 20 μm. **B** Subcellular localization of Snap23 in M II oocytes. Oocytes were immunostained with Snap23 antibody and counterstained with Hoechst. Scale bar, 20 μm. **C** Localization of Tgm2 in the zygotes fertilized from NEM-treated (10 μM), Snap23-KD, and BAPTA-treated (5 μM) oocytes. Mouse oocytes or zygotes were immunostained with Tgm2 antibody and counterstained with Hoechst. Scale bar, 20 μm.

cells were infected by P2 virus to express His-tagged proteins which were further purified by Ni affinity chromatography.

In vitro crosslinking assay

Recombinant ZP2 (2 μg) and ZP3 (2 μg) proteins were incubated with or without Tgm2 (4 μg) in the reaction buffer (50 mM Tris-HCl, pH 7.4, 5 mM $CaCl_2$) for 2 h at 37 °C. Then the reaction mixture was analyzed by immunoblotting using the antibodies for target proteins.

Statistical analysis

All percentages or values from at least three independent experiments were expressed as mean ± SEM or SD, and the number of oocytes observed was labeled in parentheses as (n). Data were analyzed by paired-samples *t-test*, which was provided by GraphPad Prism 8.0 statistical software. The level of significance was accepted as $p < 0.05$.

RESULTS

Identification of Tgm2 as a ZP binding protein

To identify the molecules that would potentially modify the ZP proteins during fertilization in oocytes, we performed immunoprecipitation followed by mass spectrometry (MS) analysis using the antibody M2c.2 which specifically recognizes the C-terminus of mouse ZP2. From the result of MS, we observed that ZP2, ZP3, and ovastacin (Astl) were abundantly present in the list (Fig. 1A), verifying the reliability of the experiment. Notably, we found that transglutaminase 2 (Tgm2), a calcium-dependent enzyme that catalyzes the transamidation of glutamine residues of a protein substrate to form intermolecular isopeptide bonds [15, 16], is a ZP2 binding protein (Fig. 1A). Furthermore, co-immunoprecipitation assay was carried out to show that Tgm2 interacted with both ZP2 and ZP3 in oocytes (Fig. 1B), indicating that Tgm2 might have a function on the ZP proteins.

We next examined the subcellular localization and expression patterns of Tgm2 at different developmental stages in oocytes and early embryos. Fluorescence imaging results revealed that both endogenous Tgm2 and exogenous Tgm2-6×HA were localized in the subcortical region of oocytes from GV (a large nucleus covered by a nuclear envelope in an oocyte arrested at meiotic prophase I) to M II stages, but almost completely disappeared in 1-cell and 2-cell embryos (Fig. 1C, S1). Consistently, the protein level of Tgm2 remained constant during oocyte

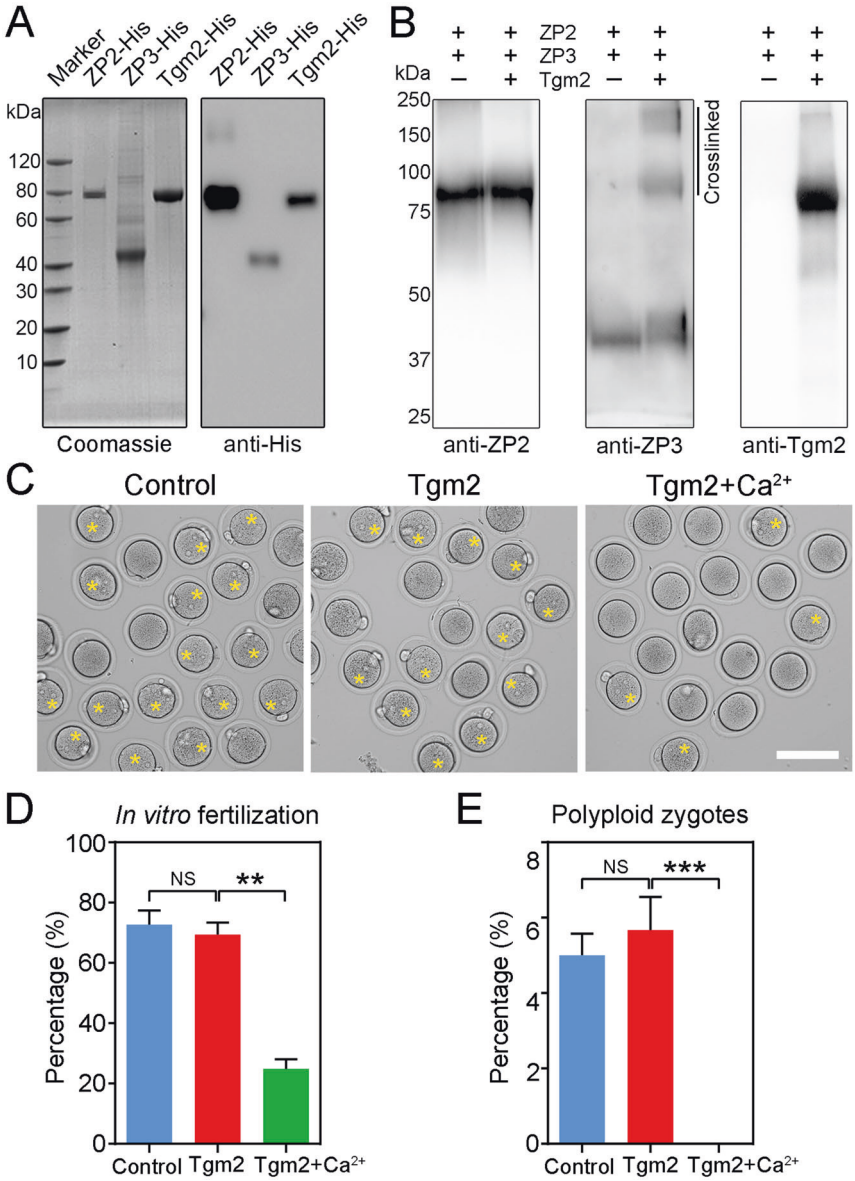

Fig. 6 Recombinant Tgm2 binds to and crosslinks ZP3 proteins in vitro. A Expression and purification of His-tagged proteins. Recombinant Tgm2, ZP2, and ZP3 proteins were expressed in Sf9 cells and purified according to the His purification procedure. Purified proteins were identified by coomassie staining and immunoblotting with His antibody. **B** In vitro crosslinking assay was performed by incubating recombinant Tgm2 with ZP2 and ZP3 proteins in the reaction buffer. After the reaction, they were immunoblotted for Tgm2, ZP2, and ZP3, respectively. **C** Representative images of in vitro fertilized oocytes in control, Tgm2 (treatment without Ca^{2+}) and Tgm2 + Ca^{2+} (treatment with Ca^{2+}) groups. Oocytes treated with recombinant Tgm2 (0.1 mg/ml) with or without 5 mM $CaCl_2$ were fertilized by sperm in vitro. **D** The fertilization rate was quantified in control ($n = 320$), Tgm2 ($n = 310$) and Tgm2 + Ca^{2+} ($n = 308$) groups. (**E**) The rate of polyploid zygotes was quantified in control ($n = 320$), Tgm2 ($n = 310$) and Tgm2 + Ca^{2+} ($n = 308$) groups. Data of (D) and (E) were presented as mean percentage (mean ± SEM) of at least three independent experiments. $^{**}P < 0.01$, $^{***}P < 0.001$.

meiosis but was dramatically reduced in 1-cell embryos as assessed by immunoblotting (Fig. 1D). These observations suggest that Tgm2 is likely to have a role during fertilization.

Tgm2 is required for post-fertilization zona block to sperm penetration and polyspermy

To investigate the exact roles of Tgm2 during fertilization, we first used its specific inhibitor LDN-27219 to treat the oocytes. In vitro fertilization assay displayed that over 40% of Tgm2-inhibited oocytes were fertilized with more than one additional sperm in the perivitelline space compare to ~20% in the controls (Fig. S2A–C). Among them, approximately 20% of Tgm2-inhibited oocytes developed to polyploid embryos while only ~5% in the controls (Fig. S2D), indicating that inhibition of Tgm2 activity leads to the defective post-fertilization zona block to sperm penetration.

To further validate the function of Tgm2 in vivo, we generated Tgm2 knockout mice by CRISPR/Cas9 technology. 49 bp nucleotides were deleted in the exon 2 of Tgm2 to create the frameshift mutation of the following sequence (Fig. S3A). Genotyping was determined by PCR and sequencing (Fig. S3B, C). Both immunostaining and immunoblotting results showed that Tgm2 was successfully ablated in the oocytes (Fig. S4). *Tgm2*-null female mice produced the normal number of ovulated oocytes (Fig. S5). In vivo fertilization experiment carried out with *Tgm2*-null female mice and wild type male mice revealed that *Tgm2*-null oocytes

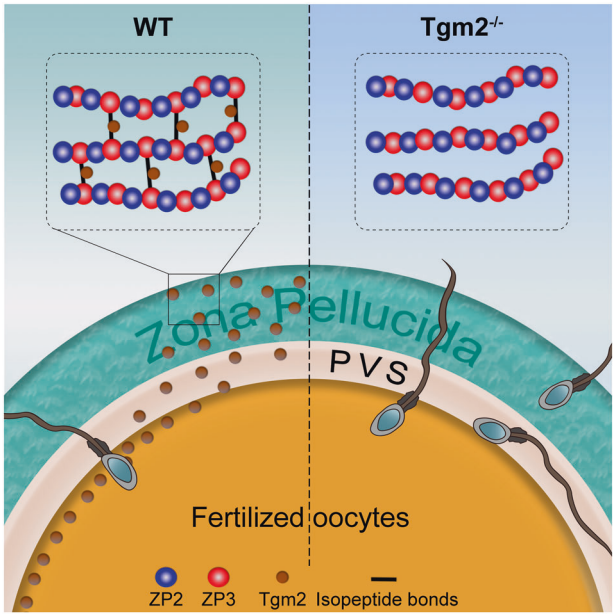

Fig. 7 Working model for the function of Tgm2 in the prevention of polyspermy. In WT oocytes, Tgm2 is exocytosed to the zona matrix triggered by fertilization and crosslinks ZP3 to result in the ZP hardening, thereby preventing additional sperm penetration through ZP and polyspermy. By contrast, in oocytes ablated of Tgm2, additional sperm continue to penetrate ZP after fertilization, which increases the number of sperm present in the perivitelline space and the occurrence of polyploid embryos.

could be normally fertilized but allowed additional sperm penetration through ZP after fertilization with a much higher frequency (Fig. 2A–C), consequently leading to the polyploid embryos and significantly reduced blastocysts as well as pups (Figs. 2D, 3).

Theoretically, restoration of protein level of Tgm2 in *Tgm2*-null oocytes could rescue the defect of post-fertilization zona block to sperm penetration. To test it, we expressed exogenous Tgm2 in the knockout oocytes. Immunostaining and immunoblotting analysis displayed that exogenous Tgm2 was correctly localized and expressed in *Tgm2*-null oocytes (Fig. S6). Following in vitro fertilization, we found that the frequency of the presence of additional sperm in the perivitelline space was prominently decreased in *Tgm2*-null oocytes after the introduction of exogenous Tgm2 (Fig. 4A–C). Accordingly, the expression of Tgm2 in *Tgm2*-null oocytes lowered the incidence of polyploid zygotes (Fig. 4A, D). As sperm binding assay demonstrated that Tgm2 did not affect post-fertilization sperm binding (Fig. S7), we conclude that Tgm2 in oocytes is required for the post-fertilization zona block to sperm penetration and polyploid embryos both in vivo and in vitro.

Fertilization triggers exocytosis of Tgm2 via SNARE pathway

To further elucidate the underlying mechanisms by which Tgm2 prevents the sperm penetration through ZP following fertilization, we first investigated how fertilization triggers the exocytosis of Tgm2 out of the oocytes. A time-course experiment showed that Tgm2 began to exocytose at ~2 h and completed prior to 3 h during in vitro fertilization (Fig. S8). It has been reported that externalization of Tgm2 does not involve the classical ER/Golgi secretion pathway, but requires membrane fusion mediated by the SNARE pathway and is stimulated by Ca^{2+} in the mitotic cells [17]. We thus tested whether this is the case in the oocytes by disrupting N-ethilmaleimide sensitive factor (NSF) and soluble NSF attachment protein 23 (Snap23), two key proteins in the SNARE pathway. Immunostaining data displayed that both NSF and Snap23 had the similar localization pattern with Tgm2 in the subcortex of M II oocytes (Fig. 5A, B). Inhibition of NSF with its specific inhibitor N-ethylmaleimide (NEM), depletion of Snap23 by RNAi, or chelation of Ca^{2+} with BAPTA all caused the persistent presence of Tgm2 in the subcortical region of zygotes (Fig. 5C), indicating that fertilization-induced Ca^{2+} alteration and SNARE pathway-involved membrane fusion mediate the exocytosis of Tgm2.

Tgm2 binds to and crosslinks ZP3 in vitro

Given that Tgm2 can covalently crosslink the extracellular matrix proteins such as collagens, fibronectin, and elastin [18], we proposed that Tgm2 is released from oocytes to the extracellular space following fertilization to crosslink ZP proteins, thereby hardening the ZP structure and preventing post-fertilization sperm penetration. To verify this possibility, we purified recombinant mouse Tgm2, ZP2, and ZP3 proteins for in vitro assays. Both coomassie blue staining and immunoblotting results verified the identity of the recombinant proteins (Figs. 6A, S9A). We validated that recombinant Tgm2 bound to ZP2 and ZP3 in vitro by immunoprecipitation experiments (Fig. S9B–D). We further documented that ZP3 instead of ZP2 proteins were crosslinked in the presence of Tgm2 as assessed by in vitro crosslinking assay (Fig. 6B). We also confirmed that recombinant Tgm2 crosslinked ZP3 in the intact ZP isolated from oocytes (Fig. S10). In addition, ZP digestion assay revealed that *Tgm2*-null oocytes had defects in ZP hardening after fertilization by showing the shorter ZP digestion time than controls (Fig. S11). However, ZP digestion time significantly increased in unfertilized aged oocytes compared to the young ones, accompanied by the reduced level of Tgm2, which implies the potential contribution of Tgm2 in the ZP hardening *via* premature exocytosis induced by the maternal aging (Fig. S12). Lastly, we showed that pre-incubation of wild-type oocytes with the recombinant Tgm2 protein inhibited the occurrence of polyspermy with a weakened fertilization rate in vitro (Fig. 6C–E). Thus, these biochemical data demonstrate that ZP3 proteins are the direct substrate of Tgm2 in vitro.

DISCUSSION

Since the first IVF birth occurred in 1978, more than 8 million babies have been born worldwide as a result of this assisted reproductive technology [19, 20]. In spite of its great clinical success, IVF is always accompanied by the abnormal polyspermy because of the dispermic oocyte penetration resulting in tripronuclear (3PN) oocytes [21, 22]. The prevention and elimination of polyspermic oocytes are critical as it has been known that significantly higher spontaneous abortions and embryonic death are expected from the transfer of triploid zygotes [23]. Post-fertilization modification of egg envelope is an evolutionarily conserved phenomenon to block polyspermy across species. This process is mediated by the exocytosis of cortical granules, an oocyte-specific secretory organelle located in the cortex of unfertilized oocytes in many invertebrates and vertebrates [24]. In fishes, cortical granule enzymes alveolin and transglutaminase have been found to function in tandem in the hardening of the egg coat [25]. In mice, ovastacin confers a transient, post-fertilization block to sperm penetration, which permits a temporal window to complete the cleavage of ZP2 to block sperm binding [26]. However, depletion of ovastacin in oocytes did not affect the expression and localization dynamics of Tgm2 (Fig. S13), suggesting that these two molecules function independently in the prevention of polyspermy. Therefore, block to sperm penetration triggered by fertilization is a process that involves multiple molecules including Tgm2, ovastacin, and other unknown ones.

Zinc-enriched vesicles in the M II egg are released as zinc sparks following fertilization to modify the structure and function of the

ZP for prevention of polyspermy [27, 28]. However, it has been reported that Zn^{2+} at physiological concentrations reversibly inhibits Tgm2 activation by competing with Ca^{2+} in vitro [29, 30]. Hypothetically, low levels of Zn^{2+} in vivo facilitate Ca^{2+}-activation of Tgm2 [29]. These complicated facts suggest that an unknown mechanism might exist in oocytes to protect Tgm2 from exposure to high levels of Zn^{2+} during fertilization.

In summary, our current findings provide genetic, cellular, and biochemical evidence revealing that Tgm2 crosslinks ZP3 to bring about the ZP hardening after fertilization, ensuring the post-fertilization block to the sperm penetration through ZP and polyspermy in mice (Fig. 7). We uncover a novel molecular mechanism and a potential target for the prevention of polyspermy in addition to the known membrane and zona blocks in mammals.

DATA AVAILABILITY

All relevant data are within the paper and its Supplementary Information files.

REFERENCES

1. Bianchi E, Wright GJ. Sperm meets egg: the genetics of mammalian fertilization. Annu Rev Genet. 2016;50:93–111.
2. Ikawa M, Inoue N, Benham AM, Okabe M. Fertilization: a sperm's journey to and interaction with the oocyte. J Clin Invest. 2010;120:984–94.
3. Bhakta HH, Refai FH, Avella MA. The molecular mechanisms mediating mammalian fertilization. Development. 2019;146:dev176966.
4. Wong JL, Wessel GM. Defending the zygote: search for the ancestral animal block to polyspermy. Curr Top Dev Biol. 2006;72:1–151.
5. Clift D, Schuh M. Restarting life: fertilization and the transition from meiosis to mitosis. Nat Rev Mol Cell Biol. 2013;14:549–62.
6. Okabe M. The cell biology of mammalian fertilization. Development. 2013;140:4471–9.
7. Gardner AJ, Evans JP. Mammalian membrane block to polyspermy: new insights into how mammalian eggs prevent fertilisation by multiple sperm. Reprod Fertil Dev. 2006;18:53–61.
8. Avella MA, Xiong B, Dean J. The molecular basis of gamete recognition in mice and humans. Mol Hum Reprod. 2013;19:279–89.
9. Li L, Lu X, Dean J. The maternal to zygotic transition in mammals. Mol ASP Med. 2013;34:919–38.
10. Fahrenkamp E, Algarra B, Jovine L. Mammalian egg coat modifications and the block to polyspermy. Mol Reprod Dev. 2020;87:326–40.
11. Bianchi E, Doe B, Goulding D, Wright GJ. Juno is the egg Izumo receptor and is essential for mammalian fertilization. Nature. 2014;508:483–7.
12. Xiong B, Zhao Y, Beall S, Sadusky AB, Dean J. A unique egg cortical granule localization motif is required for ovastacin sequestration to prevent premature ZP2 cleavage and ensure female fertility in mice. PLoS Genet. 2017;13:e1006580.
13. Avella MA, Baibakov B, Dean J. A single domain of the ZP2 zona pellucida protein mediates gamete recognition in mice and humans. J Cell Biol. 2014;205:801–9.
14. Burkart AD, Xiong B, Baibakov B, Jimenez-Movilla M, Dean J. Ovastacin, a cortical granule protease, cleaves ZP2 in the zona pellucida to prevent polyspermy. J Cell Biol. 2012;197:37–44.
15. Gundemir S, Colak G, Tucholski J, Johnson GV. Transglutaminase 2: a molecular Swiss army knife. Biochim Biophys Acta. 2012;1823:406–19.
16. Wilhelmus MM, de Jager M, Bakker EN, Drukarch B. Tissue transglutaminase in Alzheimer's disease: involvement in pathogenesis and its potential as a therapeutic target. J Alzheimers Dis. 2014;42:S289–303.
17. Zemskov EA, Mikhailenko I, Hsia RC, Zaritskaya L, Belkin AM. Unconventional secretion of tissue transglutaminase involves phospholipid-dependent delivery into recycling endosomes. PLoS One. 2011;6:e19414.
18. Belkin AM. Extracellular TG2: emerging functions and regulation. FEBS J. 2011;278:4704–16.
19. Harper JC, Schatten G. Are we ready for genome editing in human embryos for clinical purposes? Eur J Med Genet. 2019;62:103682.
20. Okabe M. Sperm-egg interaction and fertilization: past, present, and future. Biol Reprod. 2018;99:134–46.
21. Grau N, Escrich L, Martin J, Rubio C, Pellicer A, Escriba MJ. Self-correction in tripronucleated human embryos. Fertil Steril. 2011;96:951–6.
22. Chen Z, Yan J, Feng HL. Aneuploid analysis of tripronuclear zygotes derived from in vitro fertilization and intracytoplasmic sperm injection in humans. Fertil Steril. 2005;83:1845–8.
23. Evans JP. Preventing polyspermy in mammalian eggs-contributions of the membrane block and other mechanisms. Mol Reprod Dev. 2020;87:341–9.
24. Liu M. The biology and dynamics of mammalian cortical granules. Reprod Biol Endocrinol. 2011;9:149.
25. Wang Y, Chen F, He J, Xue G, Chen J, Xie P. Cellular and molecular modification of egg envelope hardening in fertilization. Biochimie 2021;181:134–44.
26. Tokuhiro K, Dean J. Glycan-independent gamete recognition triggers egg zinc sparks and ZP2 cleavage to prevent polyspermy. Dev Cell. 2018;46:627–40 e5.
27. Que EL, Bleher R, Duncan FE, Kong BY, Gleber SC, Vogt S, et al. Quantitative mapping of zinc fluxes in the mammalian egg reveals the origin of fertilization-induced zinc sparks. Nat Chem. 2015;7:130–9.
28. Que EL, Duncan FE, Bayer AR, Philips SJ, Roth EW, Bleher R, et al. Zinc sparks induce physiochemical changes in the egg zona pellucida that prevent polyspermy. Integr Biol. 2017;9:135–44.
29. Roth EB, Sjoberg K, Stenberg P. Biochemical and immuno-pathological aspects of tissue transglutaminase in coeliac disease. Autoimmunity. 2003;36:221–6.
30. Stenberg P, Roth B. Zinc is the modulator of the calcium-dependent activation of post-translationally acting thiol-enzymes in autoimmune diseases. Med Hypotheses. 2015;84:331–5.

ACKNOWLEDGEMENTS

We thank Dr. Jurrien Dean very much for providing antibodies.

AUTHOR CONTRIBUTIONS

BX designed the study; ZC, YL, YM, XD and YZ performed the experiments; ZC, YL, YM, and BX analyzed the data; ZC, YL, and BX wrote the manuscript. This work was supported by the National Key Research and Development Program of China (2021YFC2700100, 2018YFC1004002).

CONFLICT OF INTEREST

The authors declare no competing interests.

ETHICS STATEMENT

No experiments involving human subjects were performed in this study. All animal experiments in this article were approved by the Animal Research Institute Committee of Nanjing Agricultural University, China.

ADDITIONAL INFORMATION

Supplementary information The online version contains supplementary material available at https://doi.org/10.1038/s41418-022-00933-0.

Correspondence and requests for materials should be addressed to Bo Xiong.

Reprints and permission information is available at http://www.nature.com/reprints

Publisher's note Springer Nature remains neutral with regard to jurisdictional claims in published maps and institutional affiliations.